

Supporting Information

Light-Emitting Atomically Precise Nanocluster-Based Flexible QR Codes for Anticounterfeiting

Jose V. Rival,^{a,b,f} Paloli Mymoona,^{a,b,f} Rajendran Vinoth,^{b,c} A. M. Vinu Mohan,^{b,c} Edakkattuparambil Sidharth Shibu*^{a,b}

^aSmart Materials Lab, Electrochemical Power Sources (ECPS) Division, Council of Scientific and Industrial Research (CSIR)-Central Electrochemical Research Institute (CECRI), Karaikudi, 630003, Tamil Nadu, India.

^bAcademy of Scientific and Innovative Research (AcSIR)-CSIR, Ghaziabad, 201002, Uttar Pradesh, India.

^cElectrodics and Electrocatalysis (EEC) Division, CSIR-CECRI, Karaikudi, 630003, Tamil Nadu, India.

*shibuchem@gmail.com or shibues@cecri.res.in

^fAuthors contributed equally

Name	Description	Page No.
Synthetic procedure	$[Au_{22}(SG)_{18}] NC$	3
Synthetic procedure	$[Au_{25}(PET)_{18}]^- NC$	3
Synthetic procedure	$[Au_{102}(p-MBA)_{44}] NC$	3
Synthetic procedure	$[Au_{144}(PET)_{60}] NC$	4
Figure S1	UV/vis absorption and PL spectra of $[Au_{22}(SG)_{18}]$, $[Au_{25}(PET)_{18}]^-$, $[Ag_{29}(LA)_{12}]^{3-}$, $[Ag_{29}(BDT)_{12}(TPP)_4]^{3-}$, $[Au_{102}(p-MBA)_{44}]$, and $[Au_{144}(PET)_{60}] NCs$	4
Figure S2	Time-dependent PL spectra of $[Ag_{29}(BDT)_{12}(TPP)_4]^{3-}$ and $[Ag_{29}(LA)_{12}]^{3-} NCs$ under 365 nm illumination	5
Figure S3	The photograph shows the transparency of the printed band	5
Figure S4	TEM image and PL spectrum recorded from the NC-based ink	5
Figure S5	XPS spectra of P 2p, O 1s, and N 1s recorded from the printed band	6
Figure S6	EDAX spectrum and elemental composition of the printed band	6
Figure S7	Temporal-PL spectra recorded from the printed band under 365 nm illumination	6
Figure S8	UV/vis absorption spectra recorded from the printed band kept at different temperatures and the photographs of the printed band under UV light before and after dipping in liquid nitrogen	7

Figure S9	<i>Five-cycles of PL spectra recorded from the printed band at different temperatures</i>	7
Figure S10	<i>Water drop-profiles on PU-alone and NC-PU printed bands</i>	7
Figure S11	<i>Photographs showing the long-term stability of the printed band under water</i>	8
Figure S12	<i>Photographs of the printed band captured during the wincing under UV light and the photograph showing the restoring ability of printed band after stretching</i>	8
Figure S13	<i>The stress-stain curves recorded from NC-PU and PU-alone printed band</i>	8
Figure S14	<i>Photographs of the printed QR code on A4 paper under visible and UV light and the photograph of QR code-printed currency under visible light</i>	9
Figure S15	<i>Photographs of QR code-printed currency captured during folding and wetting assay under UV light</i>	9
Figure S16	<i>Photographs captured during the synthesis of $[Ag_{29}(BDT)_{12}(TPP)_4]^{3-}$ NC</i>	9
References		10

Supporting Experimental details

To find out the best NC suitable for the fabrication of the luminescent ink, we have synthesized and studied photophysical properties of a variety of NCs, including $[Au_{22}(SG)_{18}]$,¹ $[Au_{25}(PET)_{18}]^-$,^{2,3} $[Ag_{29}(LA)_{12}]^{3-}$,⁴ $[Ag_{29}(BDT)_{12}(TPP)_4]^{3-}$,⁵ $[Au_{102}(p-MBA)_{44}]$,⁶ and $[Au_{144}(PET)_{60}]$.⁷ The synthetic procedure for each NCs is shown below. In the first set of screening, $[Au_{25}(PET)_{18}]^-$, $[Au_{102}(p-MBA)_{44}]$, and $[Au_{144}(PET)_{60}]$ were eliminated out due to their poor PL. Though $[Au_{22}(SG)_{18}]$ NC showed better PL, their solubility in water reduced the importance. In this case, there is a chance to leach out NCs from the printed documents while wetting. Among $[Ag_{29}(LA)_{12}]^{3-}$ and $[Ag_{29}(BDT)_{12}(TPP)_4]^{3-}$, the second one showed better photostability and solid-state PL compared to $[Ag_{29}(LA)_{12}]^{3-}$ NC. As a result, we have finally selected $[Ag_{29}(BDT)_{12}(TPP)_4]^{3-}$ for ink fabrication. The UV/vis absorption and PL spectra of all NCs are shown in Figure S1.

Synthesis of [Au₂₂(SG)₁₈] NCs

[Au₂₂(SG)₁₈] NCs were synthesized using a reported protocol.¹ To 23 mL of Millipore water, HAuCl₄·3H₂O (10 mg/1.25 mL H₂O), and GSH (12 mg/0.75 mL H₂O) were added and vigorously stirred until the yellowish solution turned cloudy. Then, the pH of the reaction mixture was adjusted to 12 using aqueous NaOH (1 M), making the color of the solution transparent yellow. The Au-thiolate formed was further reduced by the dropwise addition of dilute aqueous NaBH₄ (3.5 mM, 0.1 mL) solution. During the first 15 min, the solution slowly turned orange. After 30 min, the pH was adjusted to 2.5 using HCl (0.33 M) to quench the BH₄⁻ activity and stirred slowly (500 rpm) at room temperature for 6 h. The solid crude product was obtained by adding 0.5 equivalent volume of methanol and subsequent centrifugation at 8000 rpm. Dried [Au₂₂(SG)₁₈] NCs were stored at 4 °C for further characterizations.

Synthesis of [Au₂₅(PET)₁₈]⁻ NCs

[Au₂₅(PET)₁₈]⁻ NCs were synthesized using a reported protocol.^{2,3} To a solution of HAuCl₄·3H₂O (20 mg/2 mL THF), TOAB (33 mg/1.75 mL THF) was added and stirred until the color turned dark red. Then, PET (34 μL; 5 mol equivalents w.r.t. gold) was added and stirred at 400 rpm for 1 h. The Au-thiolate solution formed was further reduced by injecting a freshly prepared ice-cold aqueous NaBH₄ solution (19 mg/1.25 mL; 10 mol equivalents w.r.t. gold). The mixture was stirred at room temperature for another 8-9 h to complete the reaction. Using a separating funnel, the organic and aqueous layers were separated (toluene was added for good separation), and the organic layer was washed several times with Millipore water. Excess thiol and other impurities were removed by precipitating NCs by adding methanol. This washing step was repeated three times. Insoluble Au-S polymers were removed from the crude mixture by extracting NCs in DCM. Finally, NCs were re-dispersed in acetone to remove byproducts (Au₁₄₄ NCs). Dried [Au₂₅(PET)₁₈]⁻ NCs were stored at 4 °C for further characterizations.

*Synthesis of [Au₁₀₂(*p*-MBA)₄₄] NCs*

[Au₁₀₂(*p*-MBA)₄₄] NCs were synthesized using the reported protocol.⁶ To 51.5 mL of Millipore water, methanol (75 mL), HAuCl₄·3H₂O (209 mg/10 mL methanol), and *p*-MBA (292 mg/18.43 mL of Millipore water, dissolved by adding 57 μL of 10 M NaOH) were added respectively. The reaction mixture was stirred at room temperature for 20 h resulting in a white precipitate. The Au-thiolate solution formed was further reduced by adding solid NaBH₄ (20.8 mg; 0.5 mol equivalents w.r.t. gold). The color of the solution immediately turned black, and

the mixture was stirred at room temperature for another 5 h. The solid crude product was precipitated by adding 800 mL of methanol and aqueous NH_4OAc (5 M, 40 mL) solution. The precipitate was collected by centrifuging at 3500 rpm for 5 min. The supernatant was decanted, and the precipitate was allowed to dry. To purify further, the precipitate was redissolved in Millipore water (4 mL) and aqueous NH_4OAc (2 M, 10 mL) solution, which was then reprecipitated by adding methanol (900 mL). The final product was obtained by centrifuging at 3500 rpm for 10 min. Dried $[\text{Au}_{102}(p\text{-MBA})_{44}]$ NCs were stored at 4 °C for further characterizations.

Synthesis of $[\text{Au}_{144}(\text{PET})_{60}]$ NCs

$[\text{Au}_{144}(\text{PET})_{60}]$ NCs were synthesized using the reported protocol.⁷ To a solution of $\text{HAuCl}_4 \cdot 3\text{H}_2\text{O}$ (118 mg/10 mL methanol), TOAB (190 mg/5 mL methanol) was added and vigorously stirred for 15 min until the color turned from yellow to dark red. Then, PET (213 μL ; 5.3 mol equivalents w.r.t. gold) was added to the reaction mixture, which rapidly produced white Au-thiolate. After ~15 min, it was further reduced by injecting a freshly prepared ice-cold aqueous NaBH_4 solution (113.5 mg/6 mL, 10 mol equivalents w.r.t. gold) under vigorous stirring. The color of the solution immediately turned black and stirred for 5 h to produce Au_{144} NCs as a black precipitate. Excess thiol and other impurities were removed by multiple washing with methanol. Insoluble Au-S polymers were removed from the crude mixture by extracting NCs in DCM. Finally, dried NCs were washed with acetone to remove byproducts (Au_{25} NCs). Dried $[\text{Au}_{144}(\text{PET})_{60}]$ NCs were stored at 4 °C for further characterizations.

Supporting Figures

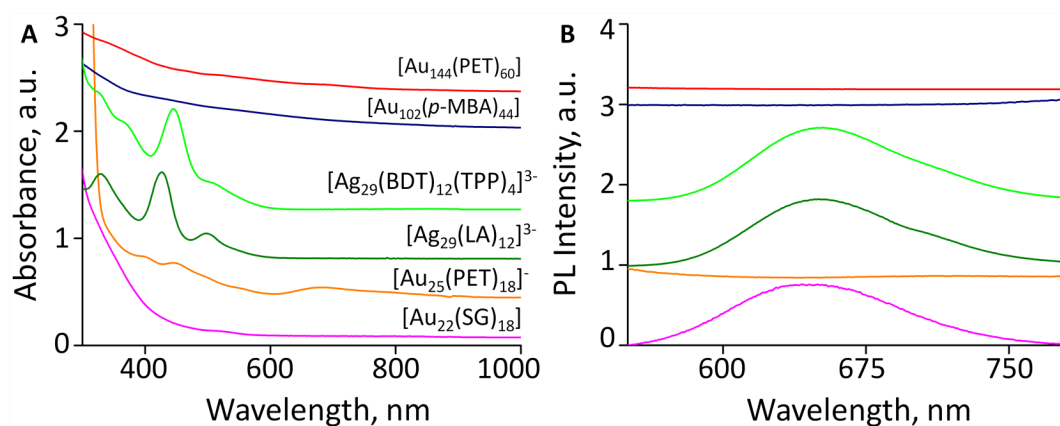


Figure S1. (A) UV/vis absorption and (B) PL spectra of $[\text{Au}_{22}(\text{SG})_{18}]$, $[\text{Au}_{25}(\text{PET})_{18}]^-$, $[\text{Ag}_{29}(\text{LA})_{12}]^{3-}$, $[\text{Ag}_{29}(\text{BDT})_{12}(\text{TPP})_4]^{3-}$, $[\text{Au}_{102}(p\text{-MBA})_{44}]$, and $[\text{Au}_{144}(\text{PET})_{60}]$ NCs.

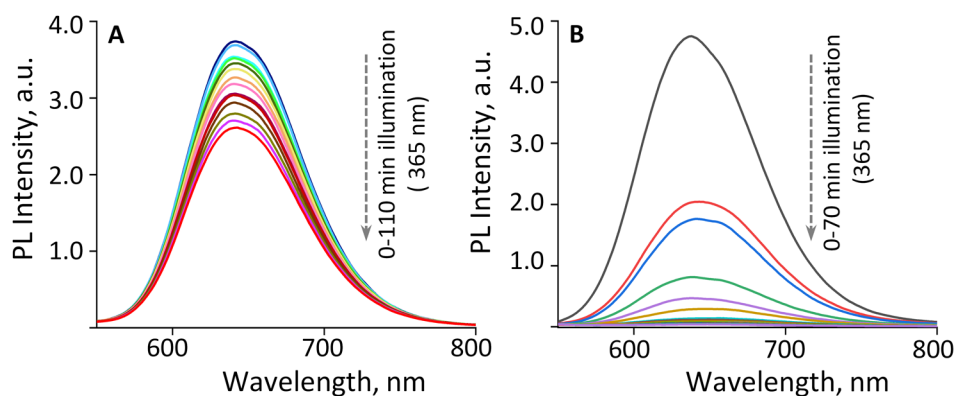


Figure S2. Time-dependent PL spectra recorded from (A) $[\text{Ag}_{29}(\text{BDT})_{12}(\text{TPP})_4]^{3-}$ and (B) $[\text{Ag}_{29}(\text{LA})_{12}]^{3-}$ NCs under 365 nm illumination.



Figure S3. The photograph shows the transparency of the printed band. Low concentration ink (7mg NC/24 mL PU) has been used in this case.

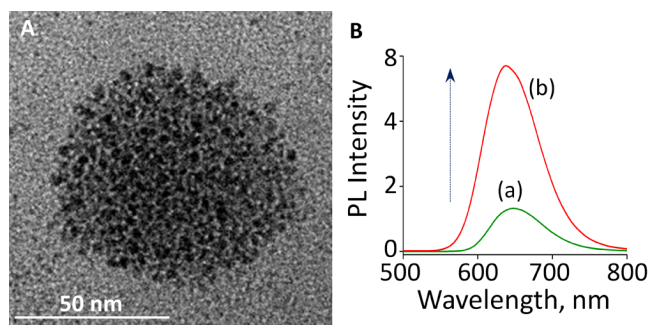


Figure S4. (A) Zoom-in and focused TEM image captured from the NC-based ink shows the self-assembly of NCs. (B) PL spectra recorded from (b) NC-based ink and (a) NC solution (same concentration) shows a four-fold enhancement for NC-based ink.

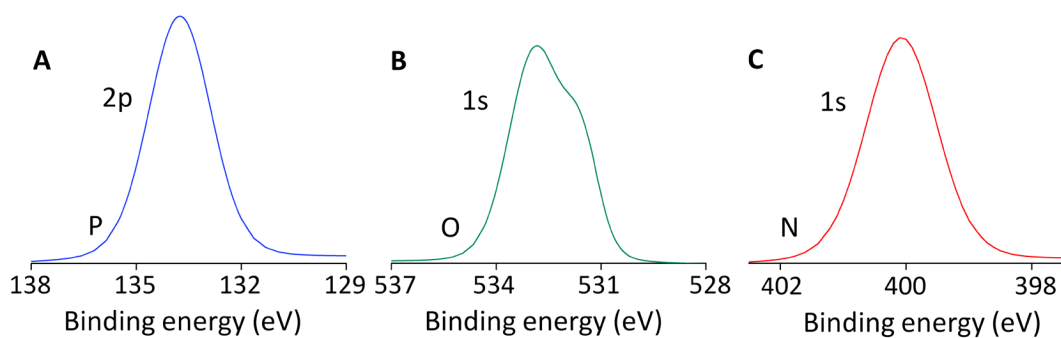


Figure S5. XPS spectra of (A) P 2p, (B) O 1s, and (C) N 1s recorded from the printed band.

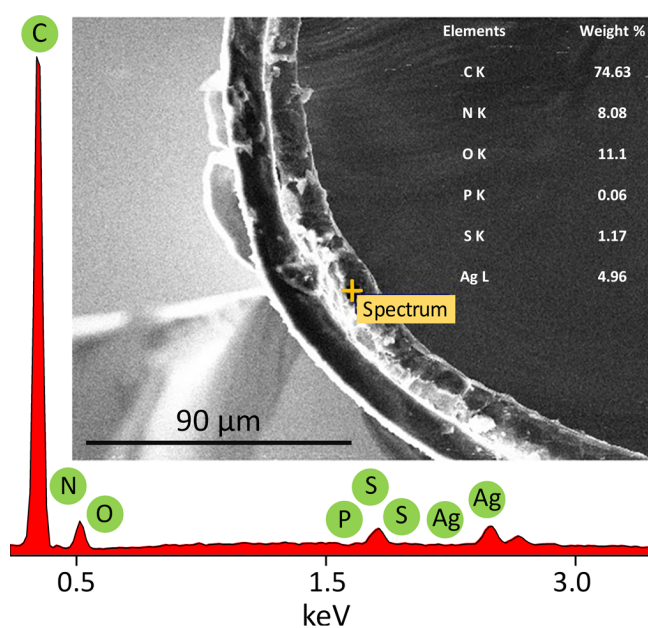


Figure S6. The EDAX spectrum collected from the printed band (shown in the inset). The elemental composition is also shown.

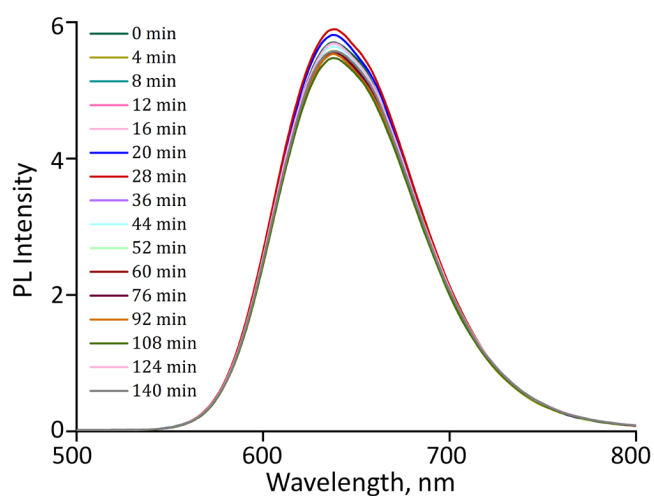


Figure S7. Temporal-PL spectra recorded from the printed band illuminated under 365 nm light.

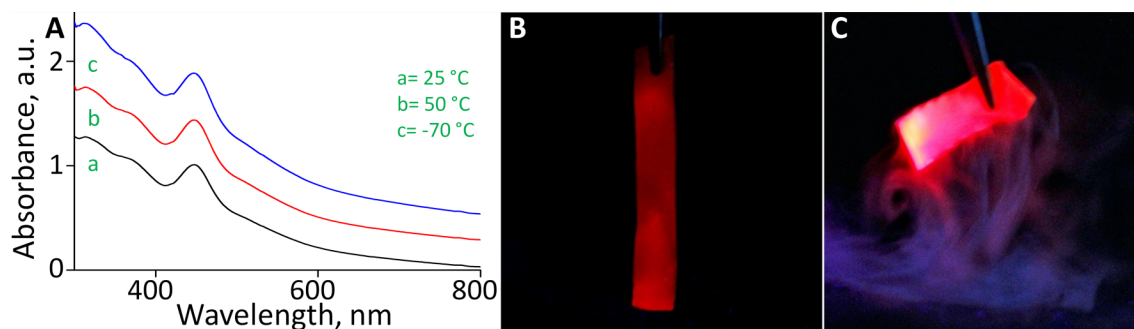


Figure S8. (A) UV/vis absorption spectra recorded from the printed band kept at different temperatures. (B and C) The photographs of the printed band under UV light (B) before and (C) after dipping in liquid nitrogen.

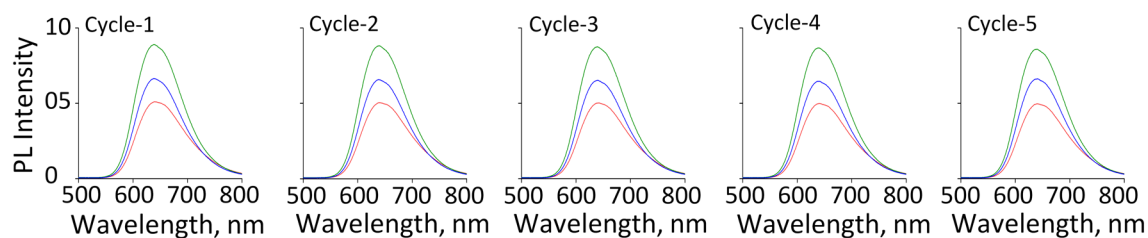


Figure S9. Five-cycles of PL spectra recorded from the printed band soaked at 50 °C (red), 25 °C (blue), and -70 °C (green).

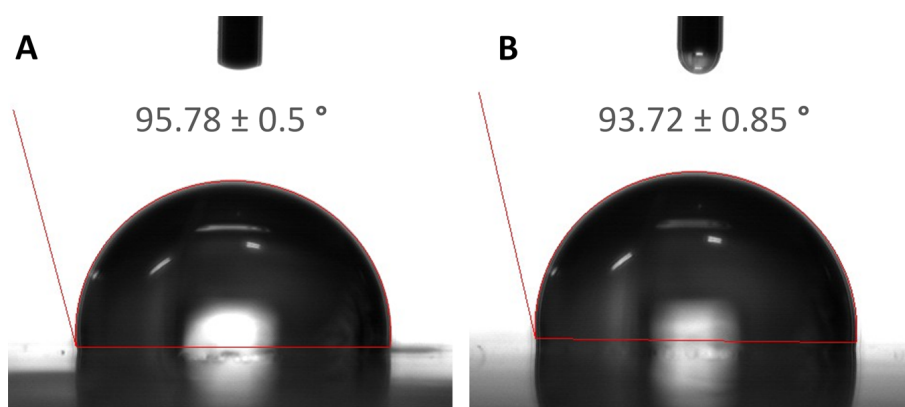


Figure S10. Water drop-profiles on (A) PU-alone and (B) NC-PU printed bands.

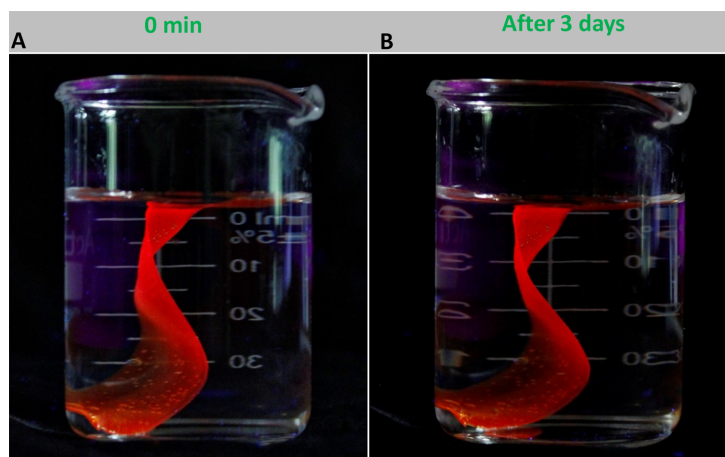


Figure S11. The photographs showing the long-term stability of the printed band under water.

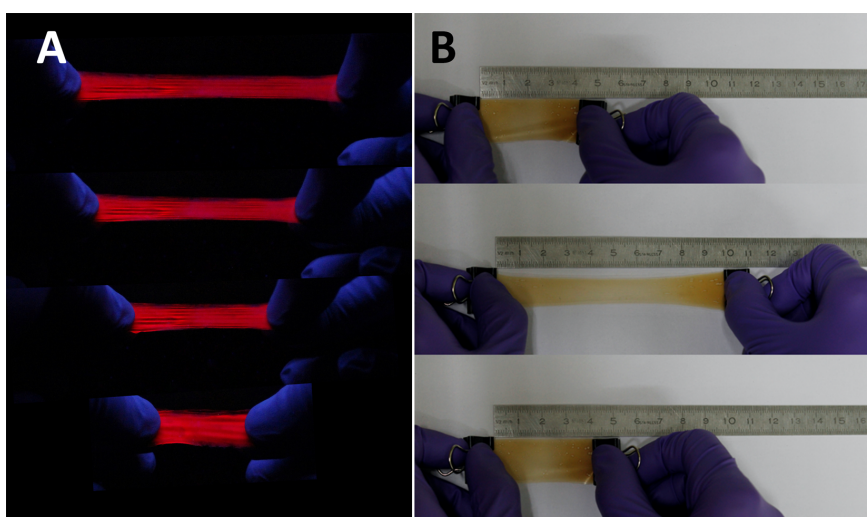


Figure S12. (A) Photographs of the printed band captured during the wincing under UV light. (B) The photographs showing the restoring ability of NC-based printed band after stretching.

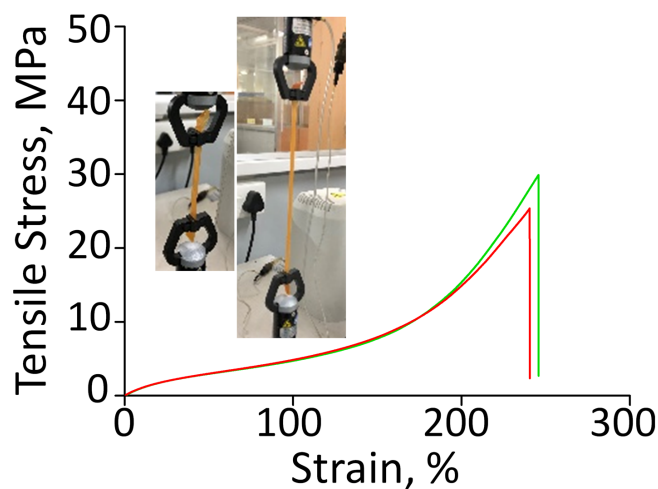


Figure S13. The stress-stain curves recorded from the NC-PU (red) and PU-alone (green) printed band. The photographs taken during the measurement are shown in the inset.

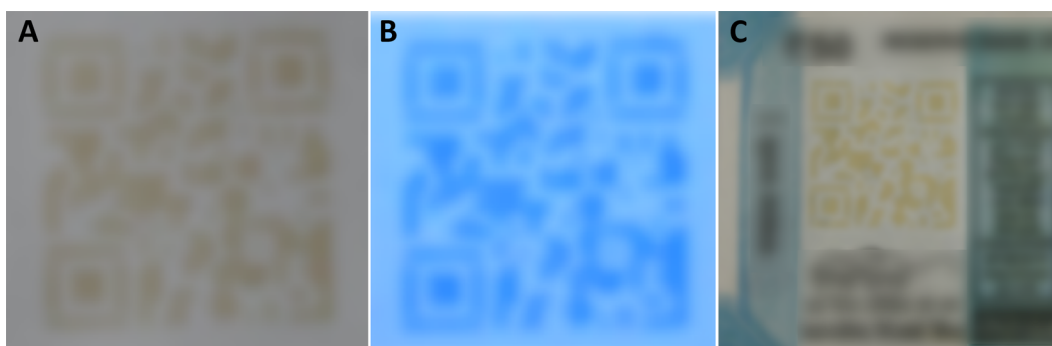


Figure S14. (A and B) Photographs of the printed QR code on A4 paper under (A) visible and (B) UV light. (C) Photograph of the QR code-printed currency (printed portion only has shown) under visible light. The photographs of the QR code and currency were blurred to avoid copyright issues.



Figure S15. Photographs of the QR code-printed currency captured during (A) folding and (B) wetting assay under UV light. The photographs of the QR code and currency were blurred to avoid copyright issues.



Figure S16. Photographs captured during the synthesis of $[\text{Ag}_{29}(\text{BDT})_{12}(\text{TPP})_4]^{3-} \text{NC}$.

References

1. Pyo, K.; Thanthirige, V. D.; Kwak, K.; Pandurangan, P.; Ramakrishna, G.; Lee, D. Ultrabright Luminescence from Gold Nanoclusters: Rigidifying the Au(I)-Thiolate Shell. *J. Am. Chem. Soc.* **2015**, *137*, 8244-8250.
2. Zhu, M.; Lanni, E.; Garg, N.; Bier, M. E.; Jin, R. Kinetically Controlled, High-Yield Synthesis of Au₂₅ Clusters. *J. Am. Chem. Soc.* **2008**, *130*, 1138-1139.
3. Rival, J. V.; Nonappa; Shibu, E. S. Light-Triggered Reversible Supracolloidal Self-Assembly of Precision Gold Nanoclusters. *ACS Appl. Mater. Interfaces* **2020**, *12*, 14569-14577.
4. Lopez, P.; Lara, H. H.; Mullins, S. M.; Black, D. M.; Ramsower, H. M.; Alvarez, M. M.; Williams, T. L.; Lopez-Lozano, X.; Weissker, H.-C.; Garcia, A. P.; Garzon, I. L.; Demeler, B.; López-Ribot, J. L.; Yacamán, M. J.; Whetten, R. L. Tetrahedral (*T*) Closed-Shell Cluster of 29 Silver Atoms & 12 Lipoate Ligands, [Ag₂₉(R- α -LA)₁₂]⁽³⁻⁾: Antibacterial and Antifungal Activity. *ACS Appl. Nano Mater.* **2018**, *1*, 1595-1602.
5. AbdulHalim, L. G.; Bootharaju, M. S.; Tang, Q.; Gobbo, S. D.; AbdulHalim, R. G.; Eddaoudi, M.; Jiang, D. E.; Bakr, O. M. Ag₂₉(BDT)₁₂(TPP)₄: A Tetravalent Nanocluster. *J. Am. Chem. Soc.* **2015**, *137*, 11970-11975.
6. Levi-Kalishman, Y.; Jadzinsky, P. D.; Kalishman, N.; Tsunoyama, H.; Tsukuda, T.; Bushnell, D. A.; Kornberg, R. D. Synthesis and Characterization of Au₁₀₂(*p*-MBA)₄₄ Nanoparticles. *J. Am. Chem. Soc.* **2011**, *133*, 2976-2983.
7. Qian, H.; Jin, R. Ambient Synthesis of Au₁₄₄(SR)₆₀ Nanoclusters in Methanol. *Chem. Mater.* **2011**, *23*, 2209-2217.